Institute for Computer Science XVII
Robotics

Bachelor's thesis

Development of a Wave Generator for Underwater Robotics

Pascal Meyer

January 2024

First reviewer: Prof. Dr. Andreas Nüchter
Advisor: Dipl.-Ing. Michael Bleier

Zusammenfassung

Unterwasser Flächen oder Objekte sind schwierig zu scannen mit den selben Methoden die außerhalb des Wassers benutzt werden. Das Hauptproblem ist die wellige Wasseroberfläche, die die Lichtwellen von Sensoren bricht. Um solche Sensoren zu erproben ist es notwendig eine Umgebung zu erschaffen in der eine wellige Oberfläche simuliert wird. Die vorliegende Arbeit behandelt das Design und den Bau von zwei Wasserwellengeneratoren für die Unterwassertestumgebung der Julius-Maximilian Universität Würzburg. Beide Wellengeneratoren erzeugen eine Wasserwelle durch eine oszillierende Bewegung, der eine durch einen auf- und abwärts beweglichen Schwimmer und der andere durch ein exzentrisch fixiertes Rohr, dass auf einer angetriebenen Achse fixiert ist. Es wurde jedoch nur einer der Wellengeneratoren, der mit dem exzentrischen Rohr, vollständig fertiggestellt. Mit Hilfe des Wellengenrators wurden drei Experimente mit verschiedenen ausgehenden Wellenlängen durchgeführt. Die resultierende Wellenhöhe des implementierten Wellengenerator wird mit der erwarteten Höhe aus der Theorie verglichen. Ein Bilderkennungsprogram wurde dafür geschrieben. Dieses Program vergleicht ein Referenzbild mit stillem Wasser und ein Bild mit den erzeugten Wellen. Die mittels des Programms gemessenen Wellenhöhen enprichen der gleichen Grössenordnung wie die der aufgestelleten Theorie. Die Resultate zeigen auch, dass der Unterschied zwischen der theoretischen und gemessenen Wellenhöhe für kleiner werdende Wellenlängen zunimmt. Die ausgehenden Wellen ensprechen keiner perfekten Sinuskurve, aber genügen für die Erprobung von Unterwassersensoren.

Abstract

Underwater surfaces or objects are difficult to scan using the same methods used outside the water. The main problem is the wavy water surface that refracts light waves from sensors. To test such sensors, it is necessary to create an environment in which a wavy surface is simulated. This work deals with the design and construction of two water wave generators for the underwater test environment at the Julius Maximilian University of Würzburg. Both wave generators create a water wave through an oscillating movement, one using an upward and downward moving plunger and the other using an eccentrically fixed roller fixed on a powered shaft. However, only the wave generator with the eccentric roller was fully completed. With the help of the wave generator, three experiments were conducted with different outgoing wave lengths. The resulting wave height of the implemented wave generator is compared with the expected height from the theory. An image recognition program was written for this purpose. This program compares a reference image with still water and an image with the generated waves. The wave heights measured by the program correspond to the same order of magnitude as those from the established theory. The results also show that the difference between the theoretical and measured wave height increases for decreasing wave lengths. The outgoing waves do not correspond to a perfect sine curve but are sufficient for testing underwater sensors.

Contents

Symbols

Symbol	Description	Unit
x	Direction of the wave propagation	m
y	Perpendicular to the x-axis and stretch the plane of the water surface	m
z	Vertical axis in the water	m
u	Horizontal water-particle velocity	$m \cdot s^{-1}$
v	Vertical water-particle velocity	$m \cdot s^{-1}$
C	Wave speed	$m \cdot s^{-1}$
L	Wave length	m
a	Amplitude of the wave	m
V_d	Displaced volume by the wave generator in half a wave length	m^2
H	Wave height, from crest to trough	m
d	Mean water depth	m
S	Stroke Length of the wave generator	m
T	Time period of one wave	s
ω	Rotation speed of the motor	RPM

Chapter 1

Introduction

This work is about the design and the construction of a wave generator for the underwater test environment described in [20]. A water wave maker is a device that displaces the water in such a way that it generates outgoing water waves of sinusoidal form (see as example Figure 1.2). The waves generated by wave generators are used for different purposes. For example the generated waves are used to analyze the effect of the ocean waves on the coastlines [21]. Another research topic is to convert the kinetic energy of the waves in electrical power [16]. Furthermore, the effect of waves on ships is also analyzed with artificially generated waves [19]. Nevertheless, a well known purpose of wave generators is for entertainment in swimming pools. Even the robotics, with the increase of automation in the past years, is taking a growing interest in underwater applications. The sensors are evolving and are facing new challenges in the underwater environment.

The robotics chair at the Julius-Maximilian University has installed an underwater test environment [20] to conduct some research on underwater robotics (See Figure 1.1). The water tank for the underwater project is a customized container that measures 7 m x 2.4 m x 2.4 m. Which corresponds to a volume of up to 40000 l of water. The water container is used to test and improve underwater sensors. For example previous research was conducted in this container to get a 3D point cloud mapunder water [20]. The next step is to make underwater 3D modeling of a surface or structure in the water from outside of the water, called bathimetric lidar. An example of a work in this domain is combining photogrammetric and radiometric methods with deep neural networks to estimate the water depth of lakes [11]. The main focus of such research is to handle the refraction of the lasers or used sensors, on the water surface. For a flat water surface a constant refraction is expected, but by involving waves the scanning needs complex adjustments. For testing such scans a wave maker is needed.

Figure 1.1: Drone image of the water tank of the Robotics chair of the Julius-Maximilian Univerität Würzburg.[20]

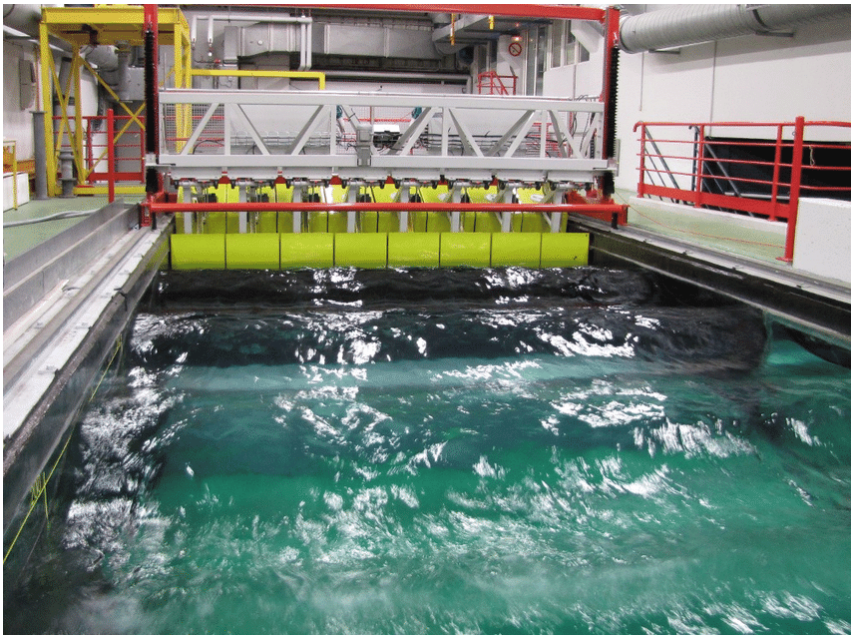

Figure 1.2: Image of the wave and current generator of the Ifremer (French Research Institute for Exploration and Exploitation of the Sea).[10]

1.1 Goal of the work

The goal of this work is to construct a wave generator for the water container of the Universität Würzburg. In the process two different wave generator types, a cylindrical plunger and an eccentric roller are developed. Both wave generator types are designed and constructed, but only the eccentric roller type is completely finished. The wave length of the outgoing wave is adjustable by setting a specific rotation steep to the actuator moving the wave generator. The produced waves are analyzed for three experiments that have different wave lengths L. The wave height H is measured with a C++ program that analyses images captured in the experiments. The measured wave height is then compared with the theory.

1.2 Outline

The first part of this work is the state of the art, where different wave generators and an equation to compute the outgoing wave height of a wave generator are presented. After that the theoretical background specific for this work is set and the equation for the wave height is specified for two different types of wave generators. The design and the construction are explained for both types. For the last part the experiments with the wave generator are conducted. The program to measure the wave height is presented and the expected. Finally, the measured values are compared to the calculated values from the theory and discussed.

Chapter 2

State of the art

In this chapter, previous research about wave generators is introduced. The first part presents different wave generator apparatus. The second part of this chapter introduces two wave equations for wave generators. The equation by Havelock [8], later reviewed by Biesel [4] and the simplified wave generator theory in shallow water by Galvin [5]. Galvin's equation is sufficient for this work. This equation is applied to two specific types of wave generators, the plunger type and the eccentric roller type.

To begin with, it is necessary to define a wave and to set a specific coordinate system for this work. A wave is a sinusoidal motion with a velocity C, a wave length L and a wave height H (defined as the distance between the crest and the trough of a wave). A wave is created by disturbing the water and the water moves away from the disturbance. For this work, we define the x-axis in the direction of the wave propagation and the y-axis perpendicular to the x-axis. The y-axis and x-axis are stretching the plane of the water surface. The z-axis is going down in the water and is perpendicular to the x-y plane.

2.1 Wave maker apparatus

Different wave generator models exist, all of which have a particular pattern of motion unique to their design. The part of the wave generator located in the water, called member, is moved with this unique pattern of motion. The member displaces a certain volume of water throughout this specific motion, creating a wave. The waveform naturally depends on the way and the amount of water that is moved. Therefore the waveform is adjustable for different applications. Biesel assumes that the ideal wave generator is the apparatus that reproduces exactly the natural motion of the water. However such an ideal wave maker is extremely difficult and expensive to construct.[4]

In the following part, four different categories of wave generators are presented. These categories are just main ideas of wave generators, which in general are quite various and are not all introduced. Each category has a variety of different patterns of motion. The first one is the piston type category (see Figure 2.1). The second one is the plunger category (see Figure 2.2), where the rigid body has different shapes, but the pattern of motion stays the same. The third category, the flap type category (see Figure 2.3), is more complex than the other ones. It has

three main aspects that define the pattern of motion. These aspects are the position and number of the articulation, the place where the moving body is fixed and the shape of the moving body. The last category yields other wave generator types (see Figures 2.5 to 2.7), which do not fit into the first three categories.

Piston type

The piston type wave generator (Figure 2.1) is an actuated body, at a perpendicular angle to the water surface, that displaces the water. In Biesel's work it yields the best results when the wave length is long in proportion to the depth. To ensure the maintenance of the piston, the movable part must prevent water leakage or the whole system must be water-resistant.[4]

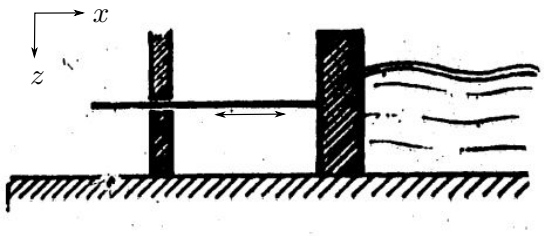

Figure 2.1: Schematic of a piston type wave generator from [4].

Plunger type

The plunger type wave maker (Figure 2.2) consists of a body with a given shape and a mechanical arm that moves that body. The motion takes place on the vertical z-axis. This wave generator is comparable to an object falling into water. The shape of the body changes the shape of the generated wave. The most common plungers have a cylindrical or prismatic shape. The maintenance is rather minimal because no parts of the articulations are in the water.[4]

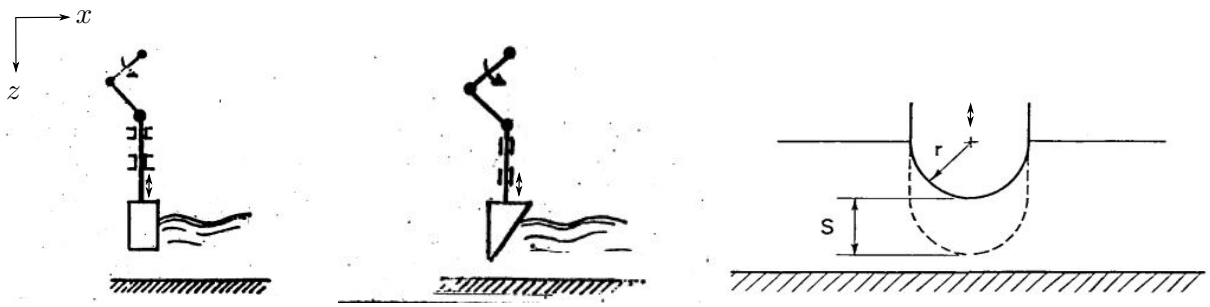

Figure 2.2: Schematics of plunger type wave makers. Left: rectangular shaped plunger from [4]. Middle: prismatic shaped plunger from [4]. Right: cylindrical shaped plunger from [5].

Flap/paddle type

The flap type wave generator consists of a wall that has an oscillating motion in the water. The motion of the flap will displace the water in the direction of wave propagation. The shape of the flap is planar or curved (see Figures 2.3). For the planar flap, it is possible to equate an analytical model of the expected wave height, but not for the curved flap. The number and position of the articulation is not fixed, but that barely modifies the shape of the wave. The way and the position that the flap is attached affects the shape of the wave. The attachment depends on whether it is attached to the bottom of the channel or not. The flap can also be placed above the water so that only the movable element is in the water (see Figure 2.3).[4]

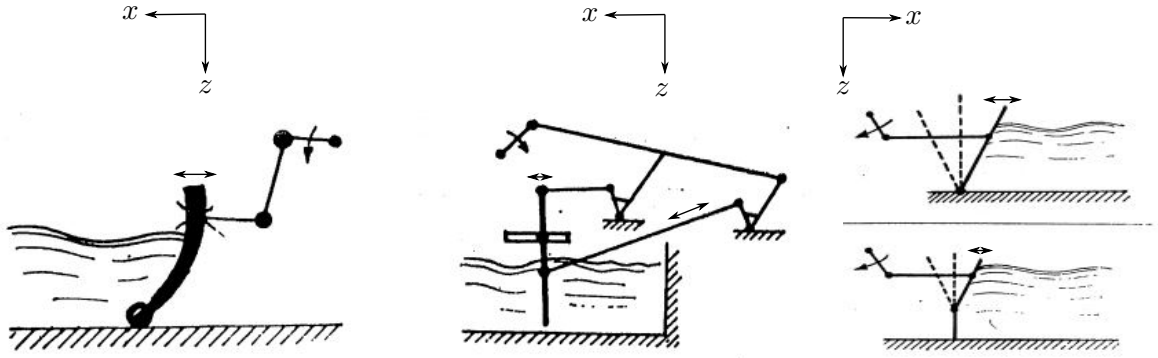

Figure 2.3: Schematics of flap type wave makers. Left: Curved flap with a double articulation attached at the bottom wave channel from [4]. Middle: plane flap with double articulation attached above the water level from [4]. Right: plane single articulated flap with adjustable attachment height from [4].

The flexible flap type wave maker (see Figure 2.4) is, in theory, the most optimal apparatus, concerning the outgoing wave form. It consists of a flexible membrane that has different oscillation amplitudes at different points of the membrane. Thus, they so recreate the natural motion of the wave. The problem with this wave maker type is the complexity of the apparatus and the reflection that it yields on the side walls of the channel. The membrane needs to be fixed to the wall to avoid leakage in the articulation.[4]

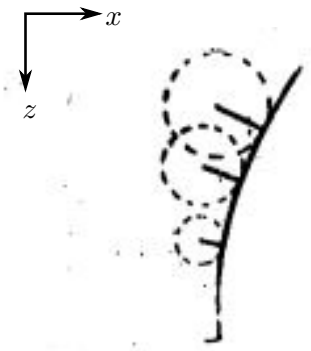

Figure 2.4: Schematic of a flexible flap type wave generator from [4].

Other types

This section presents various wave generator ideas that do not fit into the previous categories.

The serpent wave generator consists of a series of small parts that move independently of each other. The movement of each part is along the y-axis shown in Figure 2.5. The oscillation of the different parts is not in phase, and is adjustable. Therefore, it is possible to set the propagation direction of the wave. The crest of the outgoing waves is not parallel to the geometric axis of the moving parts as the majority of the wave generators.[4]

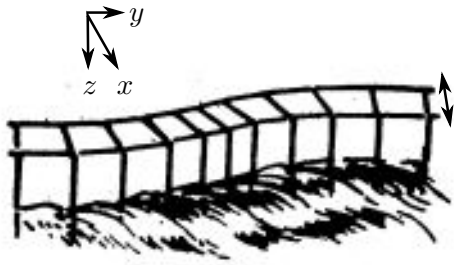

Figure 2.5: Schematic of a serpent wave generator type from [4].

The concept of the eccentric roller wave generator (see Figure 2.6) is, to eccentrically fix a cylinder or an elliptical cylinder on a rotating shaft. The volume of the roller inside the water changes with one rotation and therefore moves different volumes of water over one full rotation, creating a wave. One wave is generated for each rotation of the eccentric cylinder and two waves for the elliptical cylinder. The movement of the roller is different from the motion of a wave. So the generated waves are better with increasing distance to the roller and for a large depth wave channel.[4]

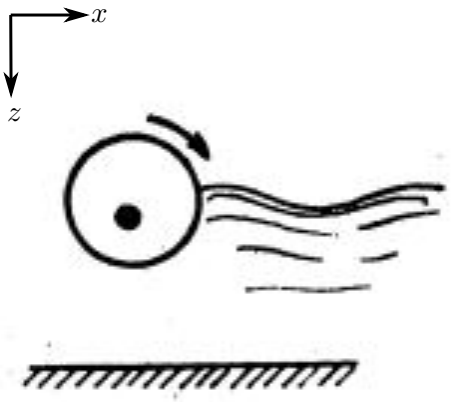

Figure 2.6: Schematic of a eccentric fixed roller wave generator type from [4].

The pneumatic wave generator (see Figure 2.7) draws in a certain volume of water and then releases it. The amount of the water that is released in a certain time and the position of the release valve in the water changes the shape of the wave. This wave generator hasn't any moving parts involved so the maintenance is simple.[4]

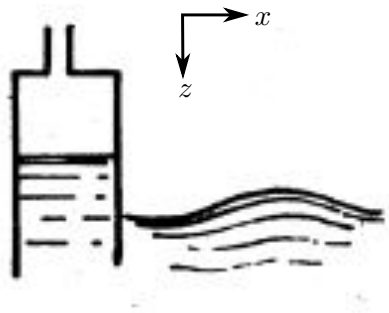

Figure 2.7: Schematic of a pneumatic type wave generator from [4].

2.2 Wave height prediction

In this part, two methods for the wave height prediction are presented, one from Havelock [8], later applied in practice by Biesel [4] and one from Galvin [5].

The method of Havelock, later Biesel, is presented at first. Based on the equation of motion of the wave in a perfect fluid by Laplace and Airy [1], Havelock worked on the problem of forced waves on the surface of the water. The solution of his work is used to describe waves produced in water by the oscillation of a solid body. Under the assumption that the water is an infinite plane or a circular cylinder. Furthermore, this theory is without the consideration of the viscosity of the water, the leakage beneath the generating member and that the water is not compressible. The movement of irrational motion of a perfect, incompressible fluid is therefore reduced to a harmonic potential function $\phi(x, z, t)$. Where the horizontal water-particle velocities u and the vertical water-particle velocities v are represented as follows:

$$u = \frac{\delta\phi}{\delta x} \quad \text{and} \quad v = \frac{\delta\phi}{\delta z} \, . \tag{2.1}$$

The boundary condition specifying a free surface at a constant pressure is set by defining the limits of the first-order equation. So second order terms of the velocities are neglected. This boundary is defined for $z = d$ and $x \geq 0$, where g is the gravity constant of Earth.

$$\frac{\delta^2\phi}{\delta t^2} + g \cdot \frac{\delta\phi}{\delta z} = 0 \tag{2.2}$$

Biesel expressed the condition that the water follows the wave generator is stated by the following equation. $k = \frac{2\pi}{T}$ and $x = \xi(z)\sin(k \cdot t)$ define the motion of the wave generator, which represents at each instance the surface of the wave generator in contact with the water.

$$\frac{\delta\phi}{\delta x} = k \cdot \xi(z)\cos(k \cdot t) \tag{2.3}$$

This boundary condition implies that the velocity of the water particles is calculated at their rest position. It is also assumed that the channel is impervious and so that: $\frac{\delta\phi}{\delta z} = 0$ for $x \geq 0$

and $z = 0$. Finally, the function ϕ and the first derivate need to be finite in the entire area of the channel. Thus, the mathematical problem is to find a function defined by a homogeneous linear equation and inhomogeneous linear boundary conditions. Havelock presents the mathematical explanation of this result [8]. With this method, it is possible to equate the movement of the waves relative to the forms of the function $\xi(z)$.[4]

Biesel analyzed different types of wave generators based on the theory of Havelock [8]. His work yields mathematical results of the problem for different wave generators and their respective $\xi(z)$ functions. He also presented the practical construction of these apparatuses.[4]

As a result, Biesel formulated a practical rule for rationally constructed wave generators without special precautions. He assumes that the wave generated by a wave maker is composed of two elements. One of the elements is a perfect wave generated by a perfect wave generator. The other element is an initial disturbance created by the wave generator, that decreases in an approximately exponential way, with increasing distance from the generator. Thus, Biesel assumes that the distance from the wave generator is required to be three times the mean water depth d to provide natural compensation for the deformation of the ideal wave form.[4]

For this work, the approximation of Galvin is sufficient, since the water channel is not ideal. Galvin proposed a theory that computes the wave height of a wave in shallow water. He considers a rigid body that generates waves by displacing a volume of water. This body has a periodic motion, with a sinusoidal form.[5]

Shallow water waves are, according to Galvin, waves where the depth of the water d is small compared with the wave length L of the wave. The linearized theory for shallow-water waves assumes that the pressure under the waves is everywhere hydrostatic. The fluid layer has a uniform mean depth, and the fluid flow is inviscid, incompressible and irrational [1]. So that the horizontal water particle velocity u is constant over the depth of the fluid. The vertical water particle velocity v is small and changes immediately as water elevation in the vertical axis. The linearized theory of shallow water is in the same order of approximation as the theory of Havelock and Biesel. The theory predicts that the shape of the wave does not change through propagation in the water with a constant depth, for the simplest periodic solution.[5]

In the following assumption, the wave generator and wave are considered as a two dimensional slice. This slice is spanned by the z-axis in the direction of the water depth and the x-axis that goes in the direction of the wave propagation (see Figure 2.8). The moving body is assumed to have an infinite length. So that the disturbance is equally distributed in the y-axis, and is so considered as infinitesimal. For a practical purpose, the example of a plunger wave maker is used to illustrate the different variables. [5]

The particle motion doesn't affect the entire tank length immediately. This includes that the disturbance travels at a known speed C away from the disturbance of the wave generator. The displaced volume by the body must therefore be stored above the mean water level, according to the fact that u is constant over the depth. Galvin shows that for a given volume with a sinusoidal movement, the volume displaced V over one entire stroke, will travel in a sinusoidal form away from the moving body. The displaced volume is the submerged volume. With the consideration that it is in a two-dimensional plane. The volume that is displaced in the half of a wave length L by the movement of the plunger is given by:

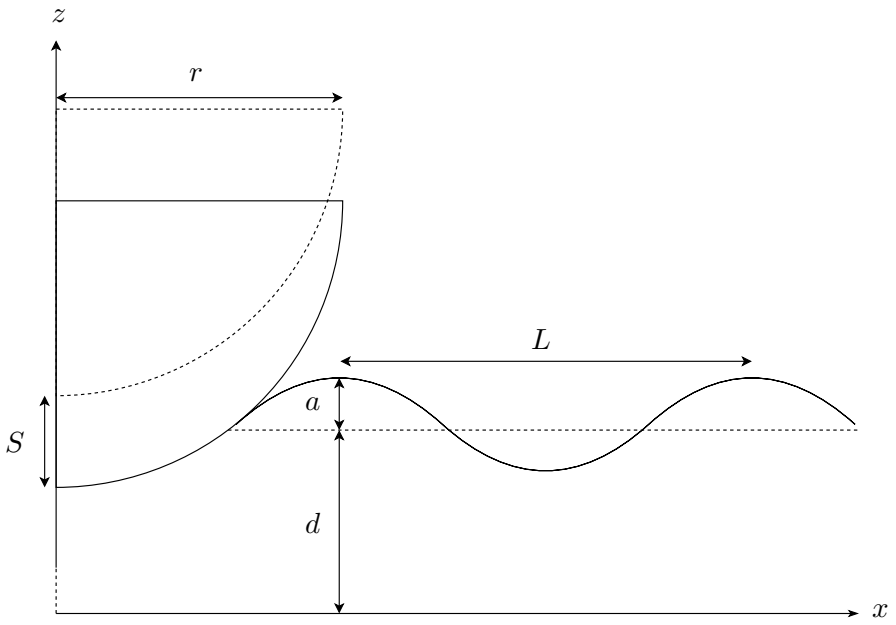

Figure 2.8: Schematics of a cylindrical plunger type wave maker.

$$\begin{aligned} V_d &= \int_0^{\frac{L}{2}} a \cdot sin(\frac{2 \cdot \pi}{L} \cdot x)\ dx \\ &= \left[\frac{L \cdot a}{2 \cdot \pi} \cdot [-cos(\frac{2 \cdot \pi \cdot x}{L})] \right]_0^{\frac{L}{2}} \\ &= \frac{L \cdot a}{2 \cdot \pi} \cdot [\ -cos(\pi) + cos(0)\ ] \\ &= \frac{L \cdot a}{\pi} .[5] \end{aligned} \tag{2.4}$$

With a being the amplitude of the wave. The displaced volume V_d is in relation with the shape of the rigid body and the stroke length S. The equation 2.4 is reformulated to give the wave height H in function of the displaced volume and the wave length. The wave height H is the distance between the crest and the trough of the wave, so two times the wave amplitude a. This leads to:

$$H(L, V_d) = 2 \cdot a = \frac{2 \cdot \pi}{L} \cdot V_d .[5] \tag{2.5}$$

With the simplified wave generator theory in shallow water of Galvin [5] it is possible to approximate the height of the generated wave for shallow water waves. For this theory, only the displaced water volume is needed, which is easy to compute for a given shape of a wave generator.

Chapter 3

Theory of physical properties of two wave generators

This chapter explains, first of all, the physical assumptions that are made to define a physical model of the wave generator as well as the expected disturbances and constraints that are encountered. The second part explains the physical theory, for the cylindrical plunger and the eccentric roller wave generators.

3.1 Physical assumptions and expected disturbances

This section explains the assumptions that are needed to build a physical model of the produced wave height and the expected disturbances on the wave form. These disturbances are determined in advance, but they are not preventable with the available means.

In order to use Galvin's simplified wave generator theory in shallow water, it is necessary to assume that the used water container satisfies the shallow water conditions mentioned in the previous section. For the means of this work, this condition is assumed to be true for the wave height equation although it is not. The disturbances on the wave caused by the problems mentioned later have a greater impact on the system and are on a larger scale.[5]

To assume an ideal wave form the length of the water tank is considered to be infinite. This leads to the most important disturbance: the wave reflection at the end of the water container which creates interference. This interference of waves colliding in opposing directions is difficult to equate since they cancel or amplify each other depending on the wave length. To avoid the initial disturbance, mentioned in the section above, the length of the channel should be three times the water depth. This condition is met if the waves are analyzed at the very end of the water container. Which is not ideal with the before mentioned reflection of the waves. In addition to that for an ideal wave the wave generator is working on the entire width of the water container, or the width of the water channel is assumed to be infinite. Furthermore, the leakage in the opposite direction of the traveling waves adds a disturbance. This leakage disturbance is not possible to avoid in reality. The shape of the walls of the water container are assumed to be a perfect plane which is not the case for the used water container. For the cylindrical plunger and eccentric roller wave generator it is assumed that the speed in the water is constant for one

oscillation and is the same as the speed of the generated waves. Also the body that is in the water and creates the waves is assumed rigid and solid. So that the shape of the moving body doesn't change. The force exerted on the body depends on the frequency and the volume that is moved in the water. Another disturbance is the decay of the vertical oscillations of a wave that propagates over a certain distance. Since the water container is short, the wave hits the wall before decaying.[4]

3.2 Physical theory

This section presents the equations to predict the wave height for a cylindrical plunger and an eccentric roller wave generator.

3.2.1 Cylindrical plunger wave maker

This part presents the theory regarding the specific case of a cylindrical plunger wave maker. The equation 2.5 that computes the expected wave height H is more detailed by specifying the displaced volume V_d in half a wave length. Since the plunger only moves water when moving downwards, the displaced volume V_d in half a wave length L is the same as the volume of the cylindrical plunger in the water at the end of the stroke. So the displaced volume V_d by the cylindrical plunger depends on the stroke length S and the radius r of the plunger. The stroke length S is defined as the depth of the movement of the plunger in the water. To equate the volume V_d the initial depth of the plunger D_i in the water must be known. Since the movement of the cylindrical body defines the wave for small and short waves, the stroke length is relatively small. The initial depth D_i is defined as $D_i \geq 0$, such that if the plunger is not in the water $D_i = 0$.

As shown in Figure 2.8 the plunger is a quarter of a circle with radius r in a two-dimensional plane. The length of the plunger in the y-axis is negligible, because of the assumption that the plunger has an infinite length. So V_d is an infinite-decimal of the volume along the y-axis, as in the equation 2.5. Another restriction of the following equation of V_d is that $S + D_i \leq r$ such that the plunger is never fully submerged. Therefore the displaced volume V_d is never greater than the volume of the plunger. For this work the plunger is assumed to be never totally submerged. The displaced volume V_d is equated:

$$\begin{aligned} V_d &= [\alpha - sin(\alpha)] \cdot \frac{r^2}{4} \\ &= \left[2 \cdot arccos\left(1 - \frac{D_i + S}{r}\right) - sin\left(2 \cdot arccos\left(1 - \frac{D_i + S}{r}\right)\right)\right] \cdot \frac{r^2}{4}\,. \end{aligned} \tag{3.1}$$

The angle α that defines the circular segment of the quarter cylinder that is in the water is equated as followed, with the height h of the plunger that is in the water in the z-axis:

$$h = r - D_i = r \cdot \left[1 - cos\left(\frac{\alpha}{2}\right)\right]\,,$$

$$\alpha = 2 \cdot arccos\left(1 - \frac{D_i + S}{r}\right) . \tag{3.2}$$

V_d is relative to the angle α which has π as maximum value with the assumed restriction. The equation for the wave height 2.5 is specified for the cylindrical plunger as:

$$H(S,L) = \frac{2 \cdot \pi \cdot r^2}{L \cdot 4} \cdot \left[2 \cdot arccos\left(1 - \frac{D_i + S}{r}\right) - sin\left(2 \cdot arccos\left(1 - \frac{D_i + S}{r}\right)\right)\right] . \tag{3.3}$$

The equation 3.3 is plotted with regards that S is not exceeding the given radius r. For this plot $r = 0.198$ m and $D_i = 0$ m are assumed.

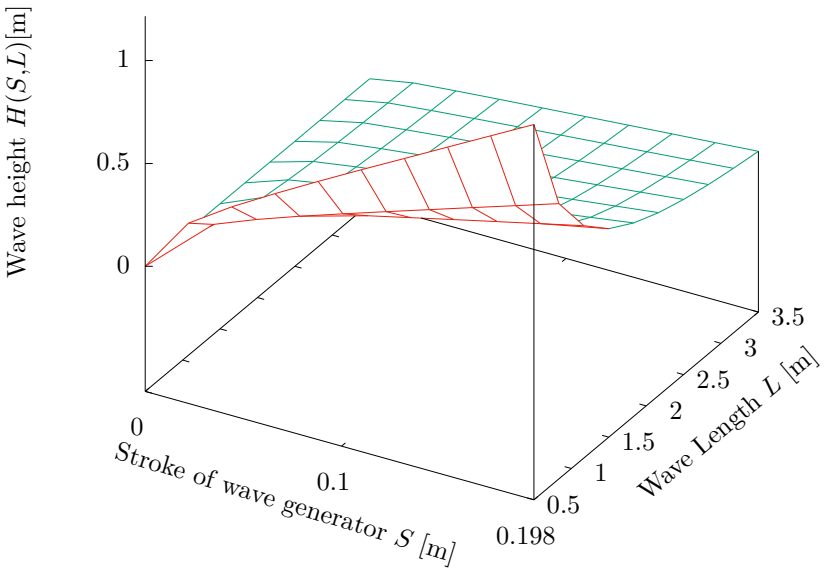

Figure 3.1: Plot of the wave height function H(S,L) (equation 3.3). The fuction shows the produced wave height H relative to the stroke length S and the wave length L of the plunger.

The stroke length S fluctuates the amount of displaced water, as shown in equation 3.1. It is evident that a longer stroke length S, with a constant plunger speed, leads to a higher H, because V_d is greater. The wave length L will modify the outgoing frequency of the displaced volume V_d as shown in equation 2.4. The wave speed C being the same as the speed of the plunger. C change the wave length, because it is defined as $C = \frac{L}{T}$ [5]. Assuming that V_d

follows the upper half of a sine-wave, the faster the speed of the plunger, the smaller is L, which leads to a greater wave amplitude a. Vice versa, the slower the speed of the plunger, the smaller is L, which leads to a smaller the wave amplitude a. So the speed of the plunger C change the wave length and so with that the wave height H. A stroke length $S = 0$ induces that the wave Height $H = 0$ what matches with the plot 3.1. And for the variable S and L, the theory is consistent with the plot in Figure 3.1. The wave height H increases with longer S and smaller L.

3.2.2 Cylindrical eccentric roller wave maker

This part presents the theory regarding the specific case of a cylindrical eccentric roller wave maker. To be able to compute an estimation about the wave height H of this wave maker with Galvin's method [5], it is necessary to compute the displaced water volume V_d in half a wave length of the eccentric cylinder. For that, it is necessary to equate a function that computes the volume V that is in the water at any moment of time in the rotation.

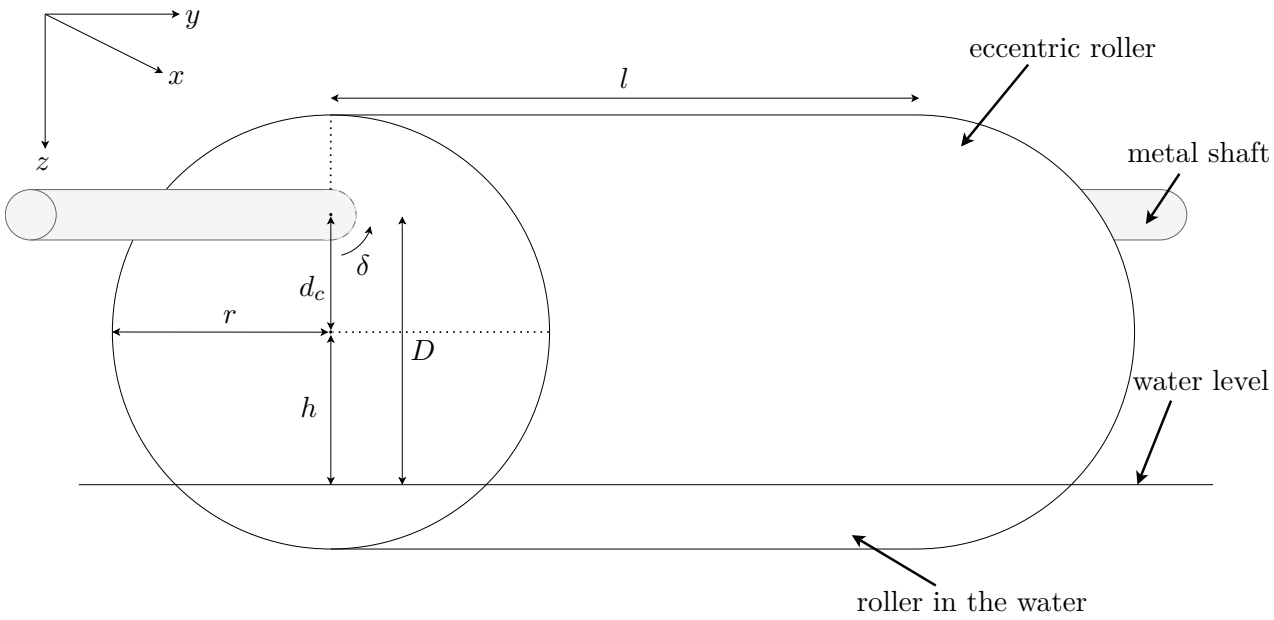

Figure 3.2: Schematics of a cylindrical roller wave maker.

With δ defined as the angle between the x-axis and the line passing through the real center of the cylinder and the eccentric fixed point of the cylinder, and d_c defined as the distance between the real center and the eccentric center, it is possible to compute the position of the real center on the z-axis. This position is described by z_{real}, the distance on the z-axis to the center of the real circle relative to center of the eccentric one at each position. Let D be the distance from the eccentric center to the water surface along the z-axis and h be the distance from the real center to the water surface, z_{real} is calculated as follows:

$$\sin\delta = \frac{z_{real}}{d_c}\,,$$
$$D = h - z_{real}\,. \tag{3.4}$$

The length of the roller in the y-axis is negligible, because of the assumption that the roller has an infinite length l. The volume V is defined as an infinite-decimal of the volume in the y-axis, as in the equation 2.5. The following equation computes the volume V of the circle that is in the water relative to the angle δ and the distance D to the water surface.

$$h = r \cdot \cos\frac{\alpha}{2}$$
$$V(\alpha) = (\alpha - \sin\alpha) \cdot \frac{r^2}{2}$$
$$V(\delta, D) = \left[2 \cdot \arccos\left(\frac{D - d_c \cdot \sin\delta}{r}\right) - \sin\left(2 \cdot \arccos\left(\frac{D - d_c \cdot \sin(\delta)}{r}\right)\right)\right] \cdot \frac{r^2}{2} \tag{3.5}$$

With r defined as the radius of the cylinder and α being the angle that defines the circular segment of the roller that is in the water, the boundaries of this function are that $-1 \geq {}^{(D-d_c\cdot\sin(\delta))}/_{r} \leq 1$, because of the arcus cosine function definition. The equation 3.5 is plotted in Figure 3.3. Therefore, the distance to the real center is set to $d_c = 0.025\,\mathrm{m}$ and the radius of the cylinder $r = 0.08\,\mathrm{m}$ which are the values later implemented in the construction of the eccentric roller. The plot in Figure 3.3 shows the displaced water V at each angle for one full rotation, and for the corresponding distance D of the roller.

The cylinder has a volume that is all the time in the water, which depends on the distance D. It is necessary to subtract the volume that is always in the water from the maximum volume V that is in the water to get the displaced volume V_d. The volume that is always in the water is computed by solving the equation 3.5 when the distance h is the highest, which is for $\delta = \frac{3\cdot\pi}{2}$. The maximum volume in the water is the solution of equation 3.5 for $\delta = \frac{\pi}{2}$. The equation to get the total displaced volume V_d for the half of the wave length comes to equate:

$$V_d(D) = V(\frac{\pi}{2}, D) - V(\frac{3\pi}{2}, D)\,. \tag{3.6}$$

The displaced volume V_d decreases for increasing distance to the water surface as shown in Figure 3.4.

With the specific displaced volume V_d the outgoing wave height H is equation 2.5 as followed:

$$H(L, D) = 2 \cdot a = \frac{2 \cdot \pi}{L} \cdot V_d(D)\,, \tag{3.7}$$

where L is in relation with the time and the outgoing wave speed C and the Periode T for one full rotation of the cylinder, $L = C \cdot T$. The resulting wave height H that the eccentric roller is producing with the relative displaced volume V_d and the distance to the water D is plotted below in Figure 3.5. The plot shows that the wave height H is decreasing with increasing L of the wave and the distance D to the water. This behavior was expected for the wave height prediction.

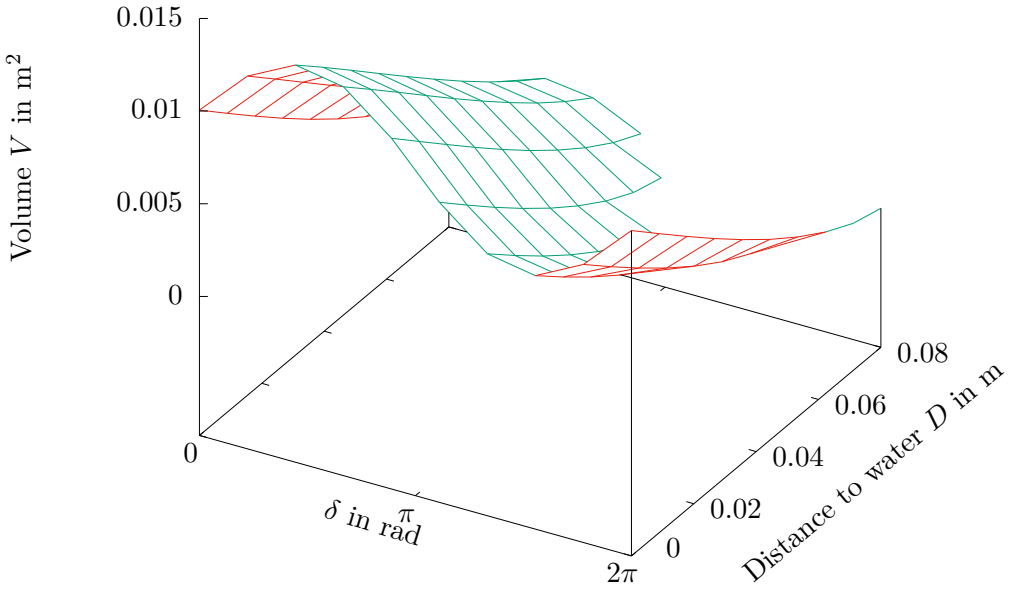

Figure 3.3: Plot of the displaced volume V relative to the angle δ around the axis and the distance to the water D being the equation 3.5.

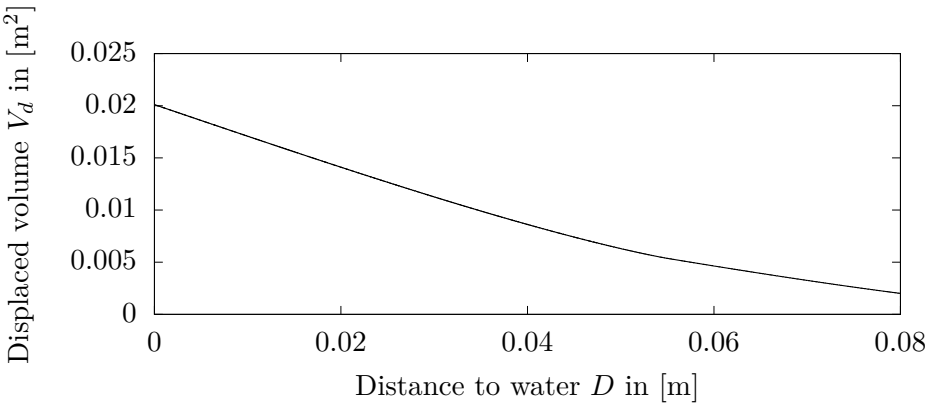

Figure 3.4: Plot of the displaced volume V_d of the eccentric roller relative to the distance d from the eccentric center and the water level (see equation 3.6).

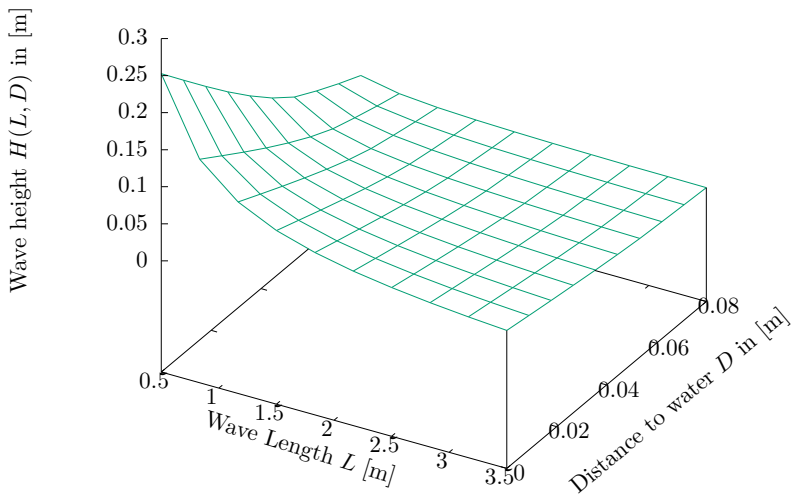

Figure 3.5: Plot of the produced wave height H (equation 3.7) with respect to the wave length and the displaced volume V_d.

Chapter 4

Design of the wave maker

In this chapter, the design of the different elements and the connection between them is presented. The constructed wave generator is at the end installed in an empty water tank. At first, a framework to support the different elements for the two wave generators is designed. The second part covers the design and implementation of two different wave makers: a cylindrical plunger and a eccentric roller. In the third part, the motor ant its controller is introduced.

4.1 Framework

To build the wave generator a framework that supports the different elements of the wave makers and the motor is needed. The constraint of this framework is that it requires to fit inside the water container. It also must be stabilized up right in the container. Besides, it needs to endure the weight, torsion, and compression forces exerted by the movements of the wave makers. The structure requires to be water resistant, especially against rust. The water container isn't ideal as well. The pressure exerted by the water bends the wall outwards. Therefore, the tank has slightly curved walls and the width, length and depth of the container are not the same everywhere.

The measurements of the water container are taken at the upper edges of it, where no pressure is exerted by the water. The exact measured dimensions of the water container are: 2350 mm large, 6700 mm long and 2380 mm high. It is also filled with 2160 mm deep water, which is not constant. The depth changes due to evaporation. The container also has a lid that has 80 mm internal height. The framework is required to fit inside the tank so that the lid is closing. At the top of the front wall of the container is an L-shaped ledge (see Figure 4.2 and 4.3b) with a vertical length of 180 mm and a horizontal length of 60 mm. On this ledge the framework is attached.

To meet the conditions, the framework consists of aluminum profiles of Type B (45 mm x 45 mm). To stabilize the structure, three pairs of adjustable feet provide a stability on the floor of the container, as shown in Figure 4.1. The top part of the framework is screwed to the L-shaped ledge with three different anchor points. As a reinforcement of this stabilization, some adjustable feet exert pressure on the side of the container and maintain the structure. These pressure feet are at the top and bottom part of the framework. The bar at the top of the structure, inside

the vertical ones, is for the motor, that it is mounted outside of the water. The constructed framework in the empty container is shown in Figure 4.2.

In order for the scaffold to withstand the different forces, three anchor points fix it. The first points are the six adjustable feet on the bottom of the container. The second one are the eight feet on the wall of the container as shown in Figure 4.3a. The third points are the three screws at the top of the framework on the L-shaped ledge, as shown in Figure 4.3b. Once the framework is set up in the container it is aligned to reduce the friction that the wave makers are exerting on it.

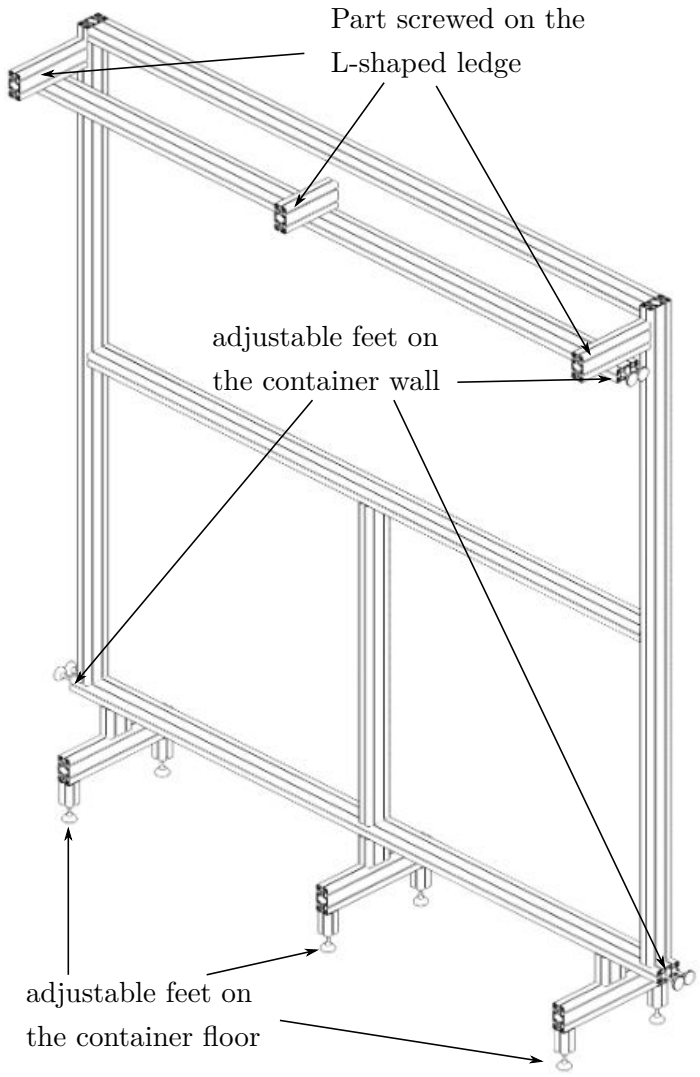

Figure 4.1: Image of the CAD Model of the framework that is installed in the water container to maintain the moving part of the wave generators.

Figure 4.2: Photo of the mounted framework in the container

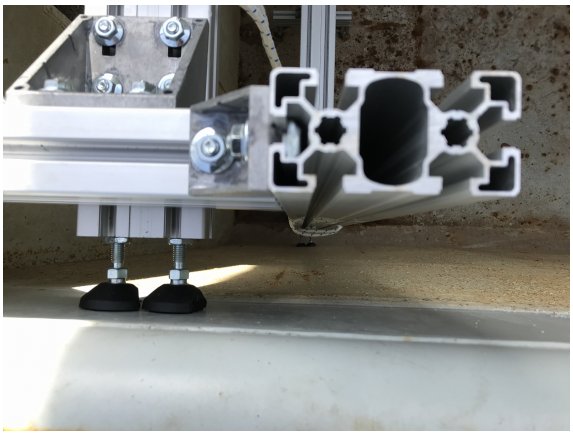

(a) Image of the adjustable feet installed on the side of the framework. The adjustable feet maintain the framework by pressure in between the walls.

(b) Image of the framework screwed on the L-shaped ledge

Figure 4.3: Images of the points that are fixing the framework in the water container.

4.2 Plunger type wave maker

In this section, the design and the installation of the cylindrical plunger type wave maker is explained. The plunger with the connection to the framework is presented at first. Then the mounting of the plunger is introduced, with the problems that occurred during the construction.

4.2.1 Plunger

The already existing plunger is integrated into the framework. A partially hollow cylindrical plunger is used. To get more weight and use less force to immerse the plunger, the hollow part is filled up with water. the filled plunger weighs about 80 kg to 100 kg. The cylindrical plunger is a quarter of a cylinder with a radius of 198 mm and a length of 2095 mm as shown in Figure 4.4.

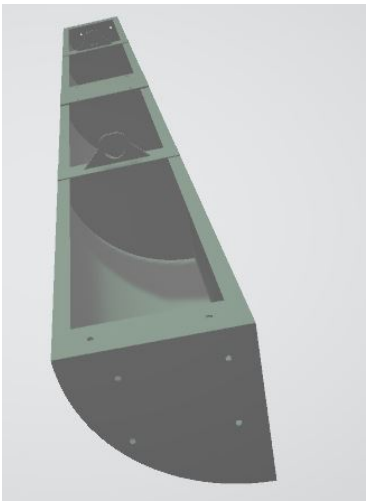

Figure 4.4: Image of the CAD model of the cylindrical plunger

The movement of the plunger is in the z-axis, and is fix in the x- and y-axis. The plunger is guided by the framework with gliders. The first approach is a glider composed of four different plastic parts on each side, see Figure 4.5b. This plastic parts being 45 mm large, 80 mm long and 5 mm thick. To connect the plunger to the eight plastic parts, two metal plates are screwed in between the plastic parts and the plunger. The plates, shown in Figure 4.5a, have small holes to screw the gliders on it and bigger ones for the plunger. The metal plate is 160 mm large, 170 mm long and 5 mm thick.

The presented setup for the connection of the plunger to the framework is not ideal, the friction that occurs is high. The four different DOLD Mechatronik glider [12] that are screwed on the metal plate are hard to perfectly align, see Figure 4.6. The force that is exerted by the metal plunger on the plastic parts, when the plunger is not perfectly horizontal, adds too much friction and restricts the movement in the z-axis. The forces exerted on the glider are loosening the screws until they fall out, as shown in Figure 4.6.

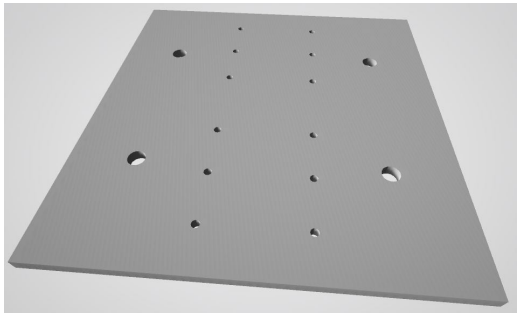

(a) Image of the CAD model of the metal plate that makes the connection between the gliders and the plunger.

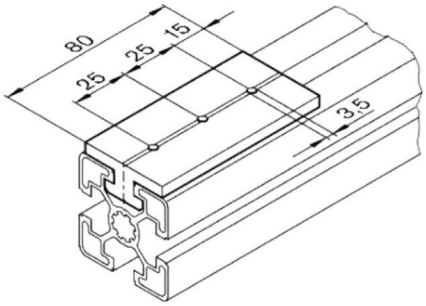

(b) DOLD Mechantronic profile glider [12] used for the connection between the aluminium profile and the metal plate.

Figure 4.5: Images of the metal plate and the glider that are making the connection between the framework and the plunger.

The second design of the glider is a 3D printed plastic piece (Figure 4.7a) which limits the amount of different parts involved in the connection. The continuity of the rails make the plunger less difficult to mount on the framework. In addition to the reduction of pieces, the thickness of the glider is reduced so that the margin between the plunger and the framework is higher. This plastic glider is screwed to the cylindrical plunger (Figure 4.7b). The plastic glider is 160 mm large, 170 mm long, 3 mm thick where the screws fix it to the metal plunger and 5 mm thick where the rails are. The plunger is mounted between the two vertical profile bars. The plunger is moving in the vertical z-axis and is fixed in the horizontal x-axis.

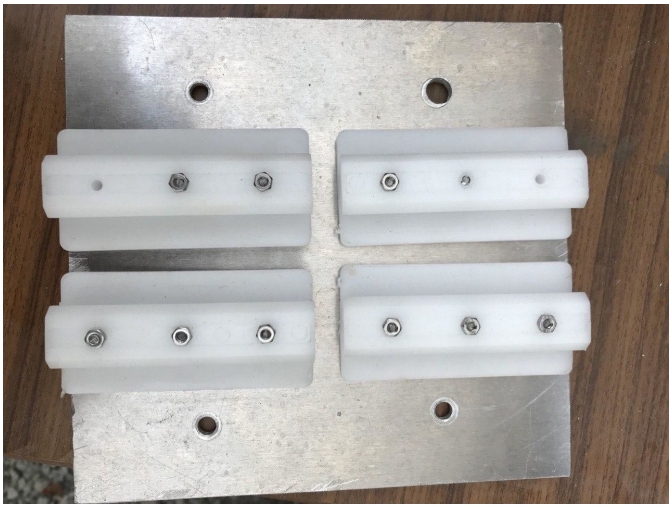

Figure 4.6: Image of the DOLD Mechatronik glider [12] that are screwed on the metal plate. This construction makes the connection between the framework and the cylindrical plunger.

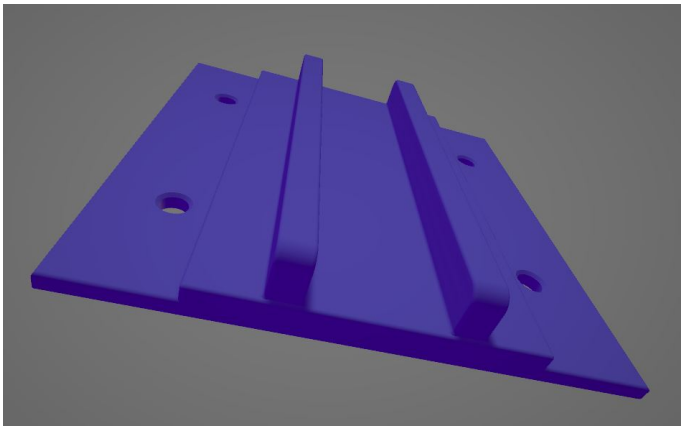

(a) Image of the CAD model of the glider.

(b) Image of the 3D printed plastic glider screwed on the cylindrical plunger.

Figure 4.7: Images of the glider used for the connection between the plunger and the framework.

4.2.2 Problems during construction

In this part the problems that occurred during the construction of the cylindrical plunger wave maker are explained. The mechanical connection from the cylindrical plunger to the framework with the glider restrains the mobility of the plunger. The length of the plunger limits the movement, as soon as one side of the plunger is higher or lower than the other one. The gliders then totally block the motion of the wave generator. The plunger is moving only if the force exerted on the plunger is exactly in the middle of the plunger. In addition to the friction occurring, the weight of the plunger is high. The motor needs to exert enough force to move the plunger on one specific location. The precise high power transmission necessary to move the plunger is not easy to achieve. The implementation of this plunger type wave maker is stopped since the dynamics required are not achieved.

To finish this project the gliding system needs improvement. An alternative solution to the gliders is to implement a system with wheels. The wheels make the transition from the plunger to the framework. The wheel based system would reduce the friction occurring on the framework.

4.3 Eccentric roller wave maker

In this section, the design and the installation of the eccentric cylindrical roller type wave maker is explained. At first the design and then the construction and implementation of the eccentric roller with the connection to the framework is presented.

4.3.1 Design

The design of the eccentric roller consist of two parts, one moving and one fixed on the framework. For the moving section of the eccentric roller a 2000 mm long metal shaft with a radius of 30 mm is mounted in between two bearings. On the shaft is a 1880 mm long pipe with a radius r of 160 mm and a thickness of 4 mm. To make the wave, the shaft is eccentrically mounted with a distance d_c of 25 mm from the center of the pipe, see Figure 4.8. Therefore the pipe rolls around an off-centered point.

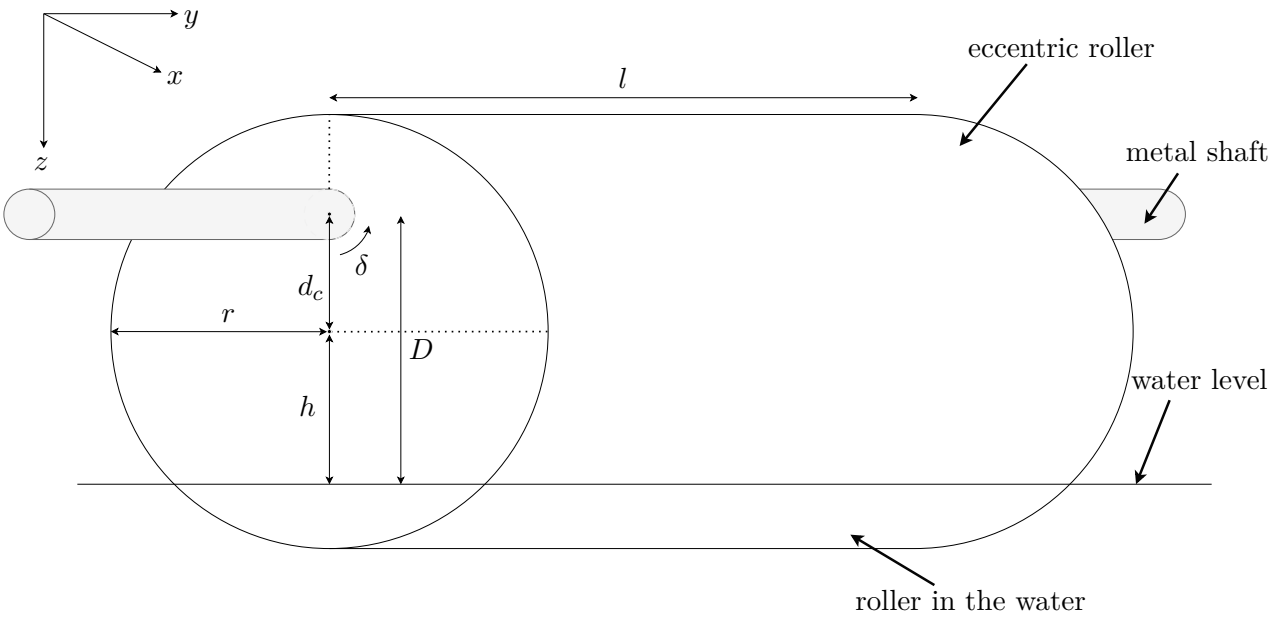

Figure 4.8: Schematics of a cylindrical roller wave maker.

To make the connection between the pipe and the shaft, three middle sockets and two end sockets are installed on the shaft. The sockets are equally spread on the pipe and reinforce the pipe against the water pressure. The end sockets also protect against the entry of water into the center of the pipe.

For the rigid part, a framework with two bearings fixes the shaft. The mount consists of four 90 mm × 45 mm type B aluminum profile pieces. A 2115 mm long profile and two 40 mm profiles mounted on the ends of the long one make the base. The bearings are mounted in between the two smaller profiles. To install the motor, one profile of a length of 30 mm is fixed on the long profile, see Figure 4.10.

This framework for the roller is connected to the main framework that is in the water container. The roller framework is mounted in between the two side profiles of the main framework (see Figure 4.2). Two metal plates on each side of the roller framework makes the connection between the two frameworks. The metal plate on the side of the main framework has screws with handles that fix the plate. This enables the height of the roller, and therefore the distance to the water surface, to be adjustable without the use of tools.

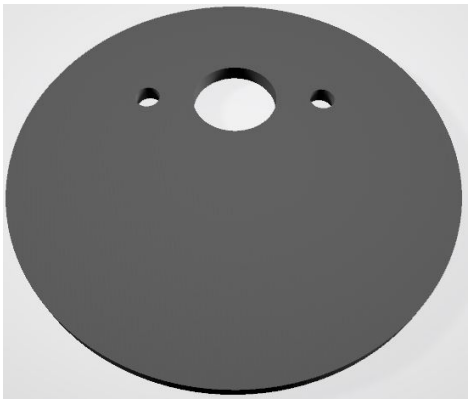

(a) Image of the CAD model of the middle sockets making the connection between the shaft and the pipe.

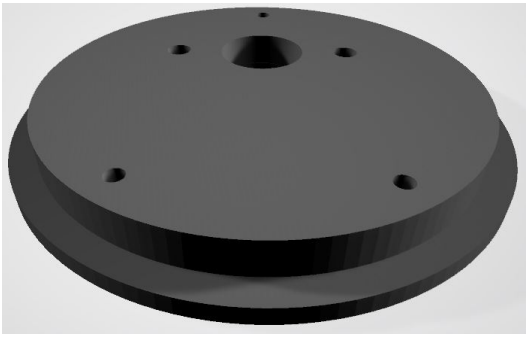

(b) image of the CAD model of the end sockets that make the connection from the shaft at the end of the pipe.

Figure 4.9: CAD of the end Sockets

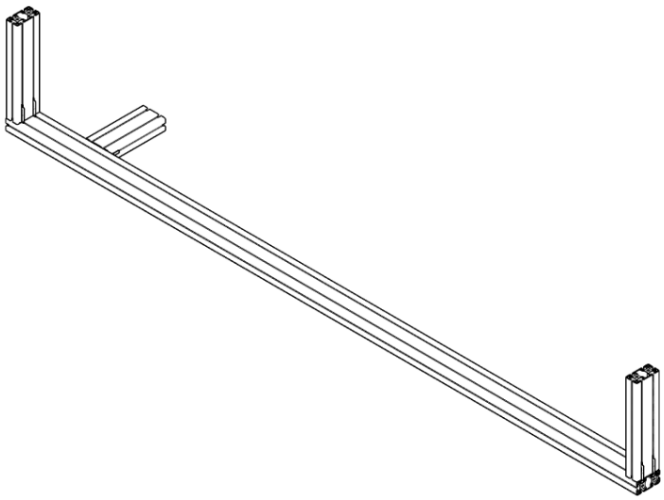

Figure 4.10: Image of the CAD model of the eccentric roller framework that is mounted in the structure inside of the water container.

4.3.2 Construction and implementation

This part is about the assembly of the eccentric roller wave generator. The first step of the construction is to laser cut the three middle and the two end sockets from a 5 mm thick Plexiglas. For the two end parts, there are three different disks that are screwed together as shown in Figure 4.11. The outer disk has a diameter of 167 mm and the two other disks have a diameter of 150 mm. Plastic washers are used on every screw involving Plexiglas to prevent damage to it.

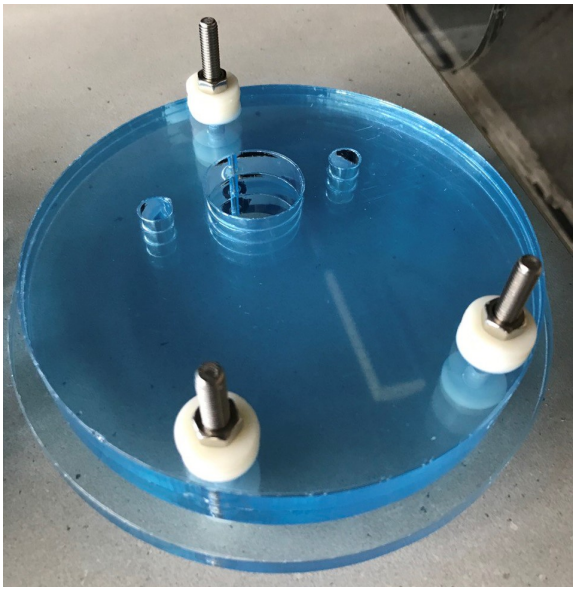

Figure 4.11: Image of a laser-cut end socket composed of three different disks screwed together.

The three middle sockets are equally distributed on the shaft. With a shift on one side, where there is 50 mm space left for the engine transmission. The middle Plexiglas sockets are fixed to the shaft with flanges as shown in Figure 4.12. The flanges ensure that the Plexiglas sockets have the same rotation speed as the shaft. The pipe is placed on the supports. The tube is gradually slided onto the plastic discs, which allows them to be aligned.

The end sockets are then mounted on the shaft and aligned with the pipe. For the transmission of the motor a 60 tooth gear is fixed on the shaft. The shaft is fixed on the side aluminum profiles of the framework with the ball bearings, see Figures 4.13. Both ends of the roller are sealed to ensure that there is no water inside the pipe. The different components such as screws, flanges, the Plexiglas end parts and the pipe are sealed together. The transition between the motor and the shaft is ensured by a gear with 60 teeth and a timing belt. The stepper motor [18] is equipped with a 15 teeth gear. The shaft has a 4:1 gear ratio. The motor is fixed on a profile as shown in Figure 4.14a, such that the timing belt is tense. The connection with the metal plates and the screw handles to the framework mounted in the tank is shown in Figure 4.14b. The construction of the eccentric roller is fully implemented in the water container as shown in Figure 4.15. The last step before conducting the experiment is to fill the water container with water.

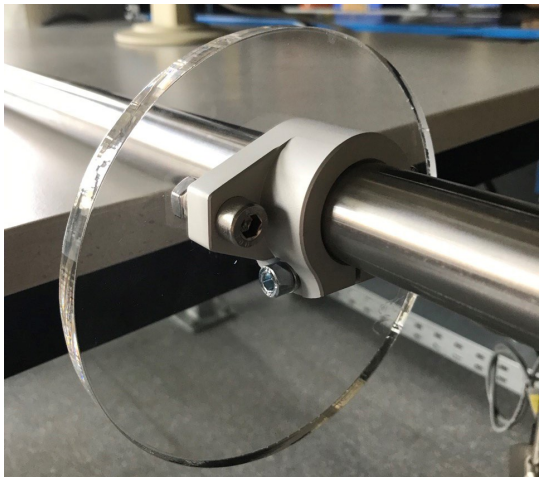

(a) Image of middle socked fixed with a flange on the shaft.

(b) Image of all middle sockets mounted on the metal shaft.

Figure 4.12: Image of the middle Plexiglas sockets mounted on the shaft.

(a) Image of the used ball bearing to fix the metal shaft in the aluminum profile framework.

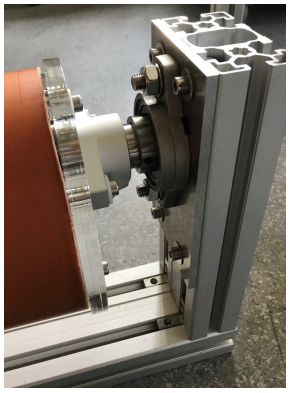

(b) Image of one end side of the pipe with the end socket fixed on the shaft that is mounted between the ball bearings.

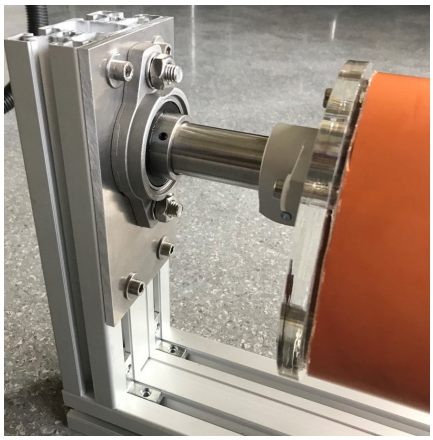

(c) Image of the other end side of the pipe with the end socket fixed on the shaft that is mounted between the ball bearings. Between this end socket and the bearing is space left for the gear that makes the transition to the motor.

Figure 4.13: Images of the ball bearings, pipes and end sockets mounted in the aluminum profile framework of the eccentric roller.

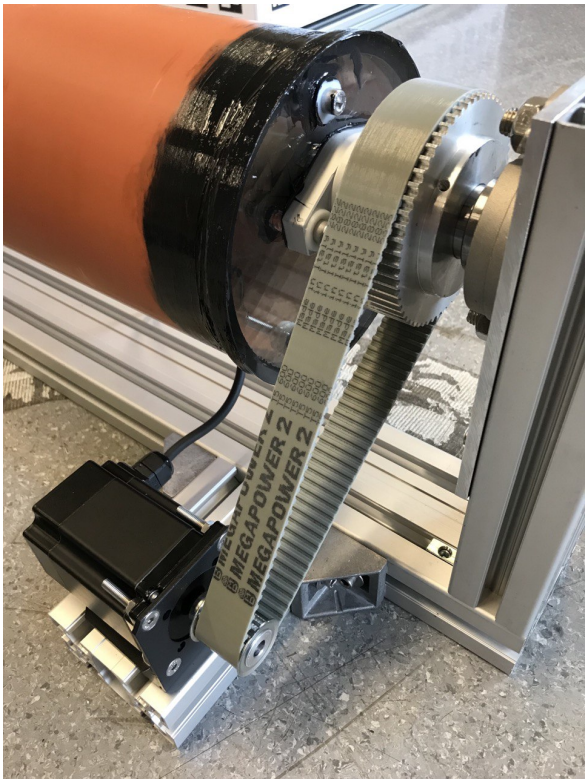

(a) Image of the stepper motor [18] and the transition with the timing belt to the gear mounted on the shaft.

(b) Connection between the framework fixed in the water container and the structure holding the eccentric roller.

Figure 4.14: Implementation of the stepper motor [18] with the transition to the shaft that is mounted in the eccentric roller framework. And the connection between the eccentric roller structure and the framework inside of the water container.

Figure 4.15: Image of the eccentric roller wave generator build in the framework that is mounted in the water container.

4.4 Actuator of the wave generator

To be able to move the membrane of the wave maker a P Series IP67 Waterproof Nema 23 bipolar stepper motor [18] with a Step angle of 1.8 ± 0.09 ° and a holding torque of 2 Nm is used. The engine is getting water droplets because of the wave generators but it is never completely submerged in the water. The motor is controlled with a digital stepper driver [17] and the steps are programed with an Arduino nano board [2]. The connections between the different components are shown in Figure 4.16.

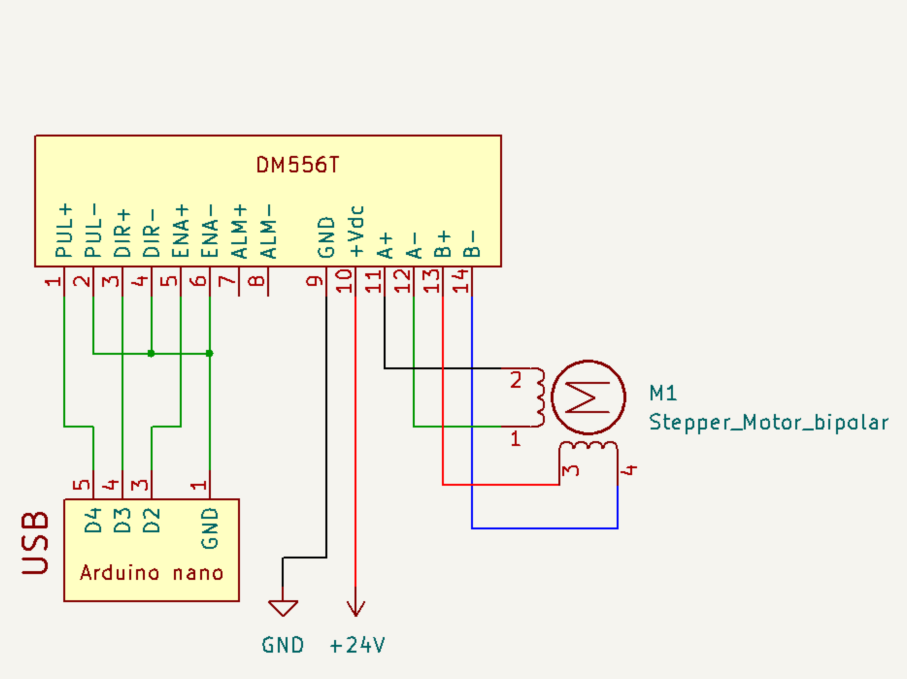

Figure 4.16: Scematics of the eletrical connection between the Arduino nano board [2], the stepper driver [17] and the stepper motor [18].

The Stepper driver's microstep resolution is set on 800 steps per revolution and the dynamic current is set to 4.5 A. The stepper driver and the Arduino nano board are put in a water sealed box that is fixed to the framework. To flash the Arduino nano board Raspberry Pi 3 board [15] is mounted in the box. The Arduino Nano board is programmed with a stepper driver library [3] to set the angular velocity of the motor.

Chapter 5

Practical work

In this chapter the constructed eccentric wave generator is tested by performing three experiments, that use different motor speeds. For each experiment a video is captured and the theoretical wave heights for the set rotation speeds of the motor ω are equated. The measurement of the produced wave height in the recorded experiments is performed with a C++ program. Finally the theoretical wave height and the measured wave height H are compared and discussed in the Results section.

5.1 Experiments

In this section the first part describes how the experiments were carried out. The second part first presents the expected wave height and then the height measured from the experiments.

5.1.1 Conduction of the experiments

The wave generator is set to three different rotation speeds ω, resulting in three experiments. One video per experiment is recorded to analyze the wave height H produced by the wave generator. The videos show the generated waves moving along the wall of the water container. To record the experiments the camera is placed on the scaffolding next to the water tank (see Figure 1.1). To calibrate the camera an Aruco marker board [7] is placed in the water along the container wall and perpendicular to the wave generator at a rough distance of 4 m. The used Aruco marker board [7] is 1.6 m long and 0.8 m large. The setup of the experiment in the water container is shown in Figure 5.1.

The rotation speed of the eccentric roller ω is set to 40 rotations per minute (RPM) for experiment one, 60 RPM for experiment two and 100 RPM for experiment three. Therefore the motor is programed to 4 times the rotation speed of the eccentric roller since the translation ratio is 4:1. For each experiment the video shows at the beginning the calm water surface. Then the motor is started and the video ends 30 s later. One image of the first arriving waves is extracted from each video displayed in Figure 5.2. To analyze the produced wave height H a reference image without waves is captured, refer to Figure 5.2a.

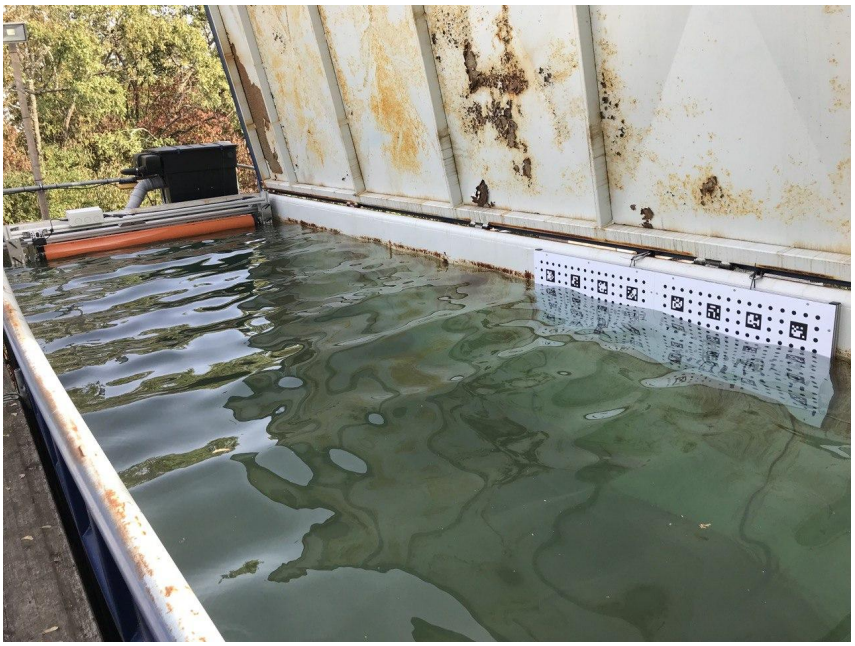

Figure 5.1: Image of the experiment setup with the eccentric roller and the Aruco marker board [7] in the water container.

(a) Image of the experiment setup without produced waves used as a reference image.

(b) Image of the experiment one extracted from the video.

(c) Image of the experiment two extracted from the video.

(d) Image of the experiment three extracted from the video.

Figure 5.2: Images of the experiments with the eccentric roller wave maker.

5.1.2 Analysis of the experiments

This part first presents the expected wave heights H based on the theory in section 3.2. The second part describes the establishment of the real wave heights H for the conducted experiments.

Theoretical approach The Experiments are conducted in a water container that contains water with a depth of roughly 2 m. The water depth to wave length ration d/L of the produced waves is bigger than $1/2$. Thus, the produced waves are considered deep water waves. The speed of the waves is therefore calculated with equation 5.2. For this equation g represents the gravitational acceleration of Earth and T the wave period, which is the time that the eccentric roller takes for one rotation. The period T is equated as:

$$T = \frac{1}{\omega \cdot \frac{1}{60}} . \tag{5.1}$$

With the equation 5.1 the velocity of the wave C is calculated as:

$$C = \frac{L}{T} = \frac{g \cdot T^2}{2\pi}, \text{ so that } L = C \cdot T .[1] \tag{5.2}$$

With a given wave length L and distance D in the water for the three different experiments the expected wave height T is computed with the equation 3.7. The displaced volume $V_d = 0.02\,\mathrm{m}^2$ is given by equation 3.6 with a distance to the water set to $D = 0$. The calculated values for each experiments are displayed in Table 5.1. The calculated values show that the expected wave height H is increasing for a decreasing wave length L and period T. Thus, the rotation speed of the motor ω changes the height H and the length L of the wave.

experiment number	ω in RPM	T in s	L in m	expected H in mm
experiment 1	40	1.5	3.51	35.8
experiment 2	60	1	1.56	80.6
experiment 3	100	0.6	0.56	224.4

Table 5.1: Table of the expected wave heights H based on the rotation speed of the motor ω for each experiment. Listed with the according period T and wave length L.

Practical approach In this part the real wave height H of the produced waves is extracted from the captured experiment videos. Therefore a C++ program was developed, which uses the OpenCV Library [13] (version 4.2), to analyze the images of the different experiments. The program calibrates the camera by detecting the board that is outside of the water and gives the wave height relative to the reference image. The written program analyses images sampled with 10 fps from the experiment videos recorded with 60 fps.

The first step of the image analysis is to detect the Aruco markers [7] on the board. Once the markers are detected the camera is calibrated relative to their position. The calibration is done for every analyzed image, since the camera was held by hand on the scaffolding outside of

the tank. An other reason of this calibration is that for bigger waves the framework vibrates due to the waves hitting the wall at the end of the container. The calibration takes the position and orientation of the Aruco markers and extracts the plane of the board in the image. The plane is then limited to the size of the board (see Figure 5.3). The calibrated images have then the size of 6400 x 3200 pixel and only show the Aruco marker board. Thus the size of one pixel is equal to 0.25 mm.

The second step is to detect the waterline. To clean up the images the Aruco markers [7] are colored white to reduce interference. The images are then filtered by keeping the part of the board above the water white and the underwater part of the image black. Only the black circles remain as interference. Therefore the black circles are now filtered out using a Hough circle detection algorithm [9]. Now the images have two parts, a white part outside of the water and the a black part inside of the water. The line that separates the white and the black part is extracted of the images and drawn in the calibrated images, as shown in Figure 5.3b. The detected water surface of the reference image and the image to analyze are drawn in the a black image of the same size as the calibrated one, see Figure 5.3a.

After getting the water level on the Aruco board the wave height H is measured. To reduce errors, all points of the detected lines that are on the same vertical axis as a black dot are removed. The program iterates true the colons of the black images and calculates the distance between the reference and the analyzed water levels. The maximum calculated values are the half of the measured wave height H of the analyzed images. The outputted distances in pixel are then multiplied by the size of 0.25 mm per pixel that was measured in the calibration. Three evaluation criteria are calculated for each experiment: the mean wave height of 60 images, the median wave height of 60 images, and one wave height from a sampled image. The three sampled images are shown in Figure 5.3. The sampled image is extracted from the 60 images used for the median and the mean wave height. The values of the three evaluation criteria are shown in Table 5.2. The results show that the measured wave height H increases for a decreasing wave length L.

The sampled images of the experiments (Figure 5.3) show that the shapes of the generated waves during one experiment are not consistent. Each produced waves has a different wave height H and form. The created program also has some errors as the Figure 5.3d shows, the detected contours near to the black dots of the marker board [7] are not always ideal. To reduce this error the program only measures the distance if there are two red points per colon. The images shown in Figure 5.3 have red contours of a bigger size for visualizing purposes.

experiment number	L in m	sampled H in mm	mean H in mm for 60 images	median H in mm for 60 images
experiment 1	3.51	28.5	28.7	27
experiment 2	1.56	44	36.5	35.5
experiment 3	0.56	71.5	60.7	58

Table 5.2: Table of the sampled, mean and median wave height H measured for each experiments

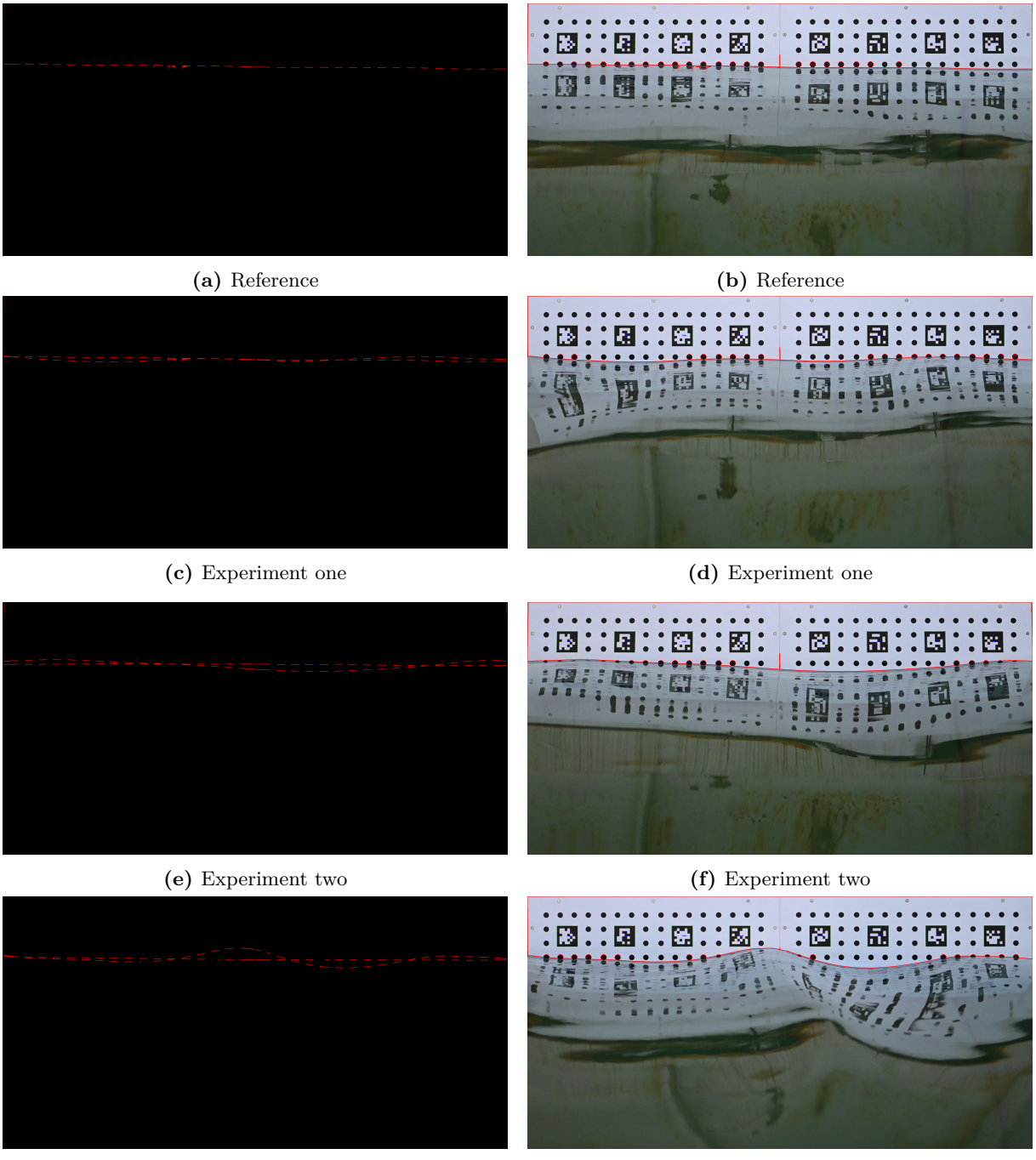

(a) Reference **(b)** Reference

(c) Experiment one **(d)** Experiment one

(e) Experiment two **(f)** Experiment two

(g) Experiment three **(h)** Experiment three

Figure 5.3: Images of the experiments video outputted by the written program. The output for each experiment are the image projected on the Aruco marker board [7], where the detected contour is shown, on the right and the measured wave level on the Aruco marker board with the reference water level on the left. The detected contours by the algorithm are depicted in red.

5.2 Results

In this part the measured wave heights H of the sampled images are compared with the expected wave heights H, based on the theory, for each experiment. The sampled heights are used from the sampled images since the shapes and wave heights are not consistent during one experiment, which has an impact on the mean and median wave heights. The sampled images are chosen from the 60 images used for each experiment by hand, and where chosen based on the clearness and ideal shape of the detected contours. The Table 5.3 shows the resulting data.

experiment number	L in m	expected H in mm	sampled H in mm	difference in mm
experiment 1	3.51	35.8	28.5	7.3
experiment 2	1.56	80.6	44	36.6
experiment 3	0.56	224.4	71.5	152.9

Table 5.3: Table of the experimental results. For each experiment the wave length L, the expected wave height H and the sampled wave height H are listed, as well as the difference between the heights.

As shown in Table 5.3 the difference of the wave heights H is increasing with a decreasing wave length L. The theoretical and measured wave height H have some errors that are important.

First the theory of Galvin [5] is for waves in shallow water and the experiments are deep water waves. This means that not all of the displaced water is assumed to create the outgoing wave. Since the water is compressible the depth of the water impacts the movements on the water. Therefore not all of the displaced water is moving in front of the wave generator, some of the water is compressed under the eccentric roller. In addition to that, water is leaking around the roller and also in the opposite x-direction of the generated wave. The wall on the backside of the wave generator also reflects the waves created on the other side of the roller. All the mentioned problems lead to a smaller measured wave height H then the expected one.

Second the position of the Aruco marker board [7] as well as the board itself is not ideal. The board is placed on the wall of the container but should ideally be placed in the middle of the wave channel. So that the disturbance of the uneven walls of the container does not impact the wave form as much. The black dots on the board create errors during the image analysis (see Figure 5.3d). In addition to that, the leakage on the side of the eccentric roller is affecting the wave form on the side of the wave channel. Therefore the measured wave height H from one outgoing wave is not always the same.

Furthermore the reflection of the waves on the wall of the water container makes the wave measurement difficult over a long time period. Only the wave height of the first waves that pass the board are measured. Also the water container begins to oscillate with the impact of the produced waves on the wall. That affects the stability of the camera as mentioned before, but also the wave form of the bouncing waves. A system to break the waves at the end of the water channel is needed to measure the wave height H over a longer time period.

Because of these error factors the measured wave height H is expected to be smaller then the theoretical wave height H. This matches the results of the conducted experiments listed in Table 5.2. The expected wave height H for experiment three with the smallest wave length L is about three times the measured value. The difference increases for a decreasing wave length L.

Chapter 6

Conclusion

In this work, a wave generator is constructed for the underwater test environment [20] of the Universität Würzburg. The plunger type wave maker design is not fully implemented, since the dynamic system has too much friction. The movement of the plunger in the framework needs improvement like a roller guided motion system. The roller system would reduce the friction, but the motion of the plunger still needs to be exactly horizontal. The second implemented wave generator is an eccentric roller type. This wave generator is fully constructed and established in the water container for operation. With this wave generator three experiments are performed. For each experiment a video of the generated waves is captured for further analysis. Then the expected wave height H calculated based on Galvin's [5] simplified wave generator theory for shallow water waves. From the videos the real generated wave height is measured by an image processing program, which is based on the OpenCV library [13]. The results show that the produced wave heights of the eccentric roller are smaller then the established wave height H of the theory, refer to Table 5.3. The expected wave height H of experiment three with the smallest wave length L is about three times the measured value. The difference between the expected and produced wave heights increases for a decreasing wave length L.

Possible causes of that difference between the expected and produced wave heights are listed below.

- The produced waves are deep water waves and are therefore not included in the linear shallow water theory of Galvin [5].
- The water tank of the underwater test environment [20] is not ideal for a wave generator. The length of the water container is to small to measure the wave sufficiently far enough from the generator [4]. In addition to that, the walls of the wave channel are not perfectly flat and the water tank vibrates due to the waves hitting the wall of the water container.
- The constructed eccentric roller wave generator is not ideal. There is leakage on the sides and the back of the eccentric roller. This problem is difficult to avoid with the used water container since a framework that maintains the wave generator is needed.
- The produced waves are reflected by the wall of the water container. The reflection of the waves acts as interference on the produced waves. The time laps without reflecting waves is therefore short. To reduce this interference a system to break the waves is required.

- The Aruco marker board [7] itself and the its position is not ideal. The optimal placement of the board is in the middle of the wave channel and not on the wall of the container as in this work. Furthermore the black dots create errors during the image analysis and are therefore ignored. This impacts the results of the program.

The above mentioned disturbances also lead to uneven waves. The wave form and height for one specific wave length L is not the same for every wave. The measurement of the wave height H needs to be done for a longer time period, which is not possible with the current setup due to the reflection on the wall of the water container.

Future work are concerned with the inclusion of a control system over the produced wave height. It is necessary to implement a closed loop control system with a sensor measuring the wave height in real time. Current problems for closed loop control pose the reflecting waves, that are increasing or decreasing the wave height of the outgoing waves. Nevertheless, even with the current setup the average wave height is controllable over a certain time. For maintenance purposes, the actuator speed should be accelerated or slowed down instead of just starting to turn at a certain speed and then stopping abruptly. With the current wave generator setup this would lead to interference of waves with different wave heights and lengths. In order to achieve this slower acceleration the waves need to break at the end of the channel.

In the end the goal of this work is to create an environment to test sensors with the produced waves. For this purpose is not necessary to achieve ideal waves. The constructed wave generator produces waves whose shape is sufficient for this purpose.

The purpose of the wave generator is to perform lidar bathimetric experiments. Therefore, as an outlook, the work of O. Oreifej, G. Shu, T. Pace and M. Shah [14] that is dealing with the reconstruction of an image which is distorted by water waves is of interest. In this paper the Fluidity algorithms [6] takes a video of an object distorted by the movement of water waves and restores the shape of that object. The implemented algorithms of the work [14] are tested on the experiment videos made with the constructed wave generator. The goal of these algorithms, in this work's application, is to reconstruct the Aruco marker board [7] and the black dots that are distorted in the water. The Fluidity algorithms are used on the following two different videos, the video of the water surface without produced waves (see Figure 6.1) and the video of experiment three (see Figure 6.2).

The output of the Fluidity algorithms [14] for the video without produced waves 6.1b shows that the Aruco marker board that is in the water is reconstructed without distortion. For the video from experiment three the reconstruction is not as good as without waves. The reflection of the Aruco board [7] and the black dots in the water makes the reconstruction of the submerged part of the board difficult. The use of videos with less reflection is necessary to improve the results of the reconstruction. New videos from directly above the water surface should improve the output of the Fluidity algorithms.

(a) Image extracted from the video of a water surface without produced waves that is used in the Fluidity program [6].

(b) Resulting image with 10 iterations of the Fluidity algorithm [6] with a video of a water surface without produced waves as input

Figure 6.1: Example of the Fluidity algorithm [6] on waves from experiment one.

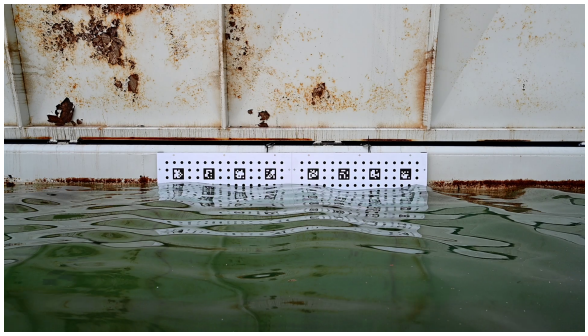

(a) Image extracted from the video of experiment three that is used in the fluidity program [6].

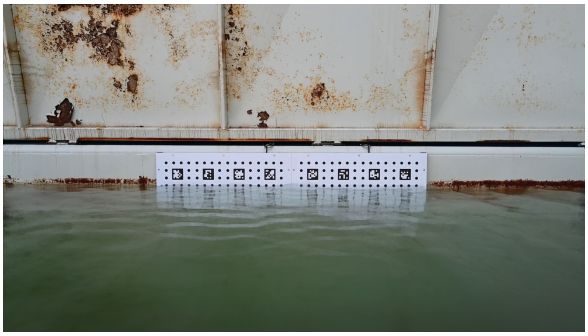

(b) Resulting image with 10 iterations of the Fluidity algorithm [6] with a video of the waves from experiment three as input.

Figure 6.2: Example of the Fluidity algorithm [6] on waves from experiment three.

Bibliography

[1] George Biddell Airy. *Tides and waves*. B. Fellowes, 1845.

[2] Arduino. Arduino nano. https://docs.arduino.cc/hardware/nano, accessed: 10.12.2023.

[3] Arduino. Stepper driver library. https://www.arduino.cc/reference/en/libraries/stepperdriver/, accessed: 10.12.2023.

[4] F. Biesel. A theoretical study of a certain type of wave generator. *La Houille Blanche, No. 4, pp. 475-496. (Page references in text refer to translation of Meir Pilch published in:Laboratory Wave generating Apparatus, St. Anthony Falls Hydraulic Laboratory Report No. 39, 1954.)*, 1951.

[5] Jr. C. J. Galvin. Wave Height Prediction for Wave Generators in Shallow-Water. *Tech Memo 4, U.S. Army, Coastal Engineering Research center*, March 1964.

[6] Aalto University 2016 Developed by Team Fluidy. Fluidity - video processing for seeing through water. https://github.com/rkheikkila/fluidy, accessed: 5.1.2024.

[7] S. Garrido-Jurado, R. Muñoz-Salinas, F.J. Madrid-Cuevas, and M.J. Marìn-Jimènez. Automatic generation and detection of highly reliable fiducial markers under occlusion. *Pattern Recognition*, 47(6):2280–2292, 2014.

[8] T. H. Havelock. Forced surface-waves on water. *The London, Edinburgh, and Dublin Philosophical Magazine and Journal of Science, s. 7, v. 2, pp. 569-576*, 1929.

[9] J. Illingworth and J. Kittler. The adaptive hough transform. *IEEE Transactions on Pattern Analysis and Machine Intelligence*, PAMI-9(5):690–698, 1987.

[10] B. Mallat, G. Germain, J.Y. Billard, B. Gaurier, J.V. Facq, and T. Bacchetti. A 3d study of the bubble sweep-down phenomenon around a 1/30 scale ship model. *European Journal of Mechanics-B/Fluids*, 72:471–484, 2018.

[11] Gottfried Mandlburger, Kölle Michael, Nübel Hannes, and Soergel Uwe. Bathynet: A deep neural network for water depth mapping from multispectral aerial images. *PFG Journal of Photogrammetry, Remote Sensing and Geoinformation Science*, April 2021.

[12] DOLD Mechatronik. Gleiter glatt b-typ nut 10. https://www.dold-mechatronik.de/Gleiter-glatt-B-Typ-Nut-10, accessed: 30.11.2023.

[13] OpenCV. Opencv library. https://opencv.org/, accessed: 10.1.2024.

[14] Omar Oreifej, Guang Shu, Teresa Pace, and Mubarak Shah. A two-stage reconstruction approach for seeing through water. In *CVPR 2011*, pages 1153–1160. IEEE, 2011.

[15] Raspberry Pi. Raspberry pi 3 model b. https://www.raspberrypi.com/products/raspberry-pi-3-model-b/, accessed: 23.12.2023.

[16] Abidur Rahman, Omar Farrok, Md. Rabiul Islam, and Wei Xu. Recent progress in electrical generators for oceanic wave energy conversion. *IEEE Access*, 8:138595–138615, 2020.

[17] STEPPERONLINE. Digital stepper driver 1.0-4.5 A 18-50 VDC for nema 17, 23, 24 stepper motor. https://www.omc-stepperonline.com/digital-stepper-driver-1-0-4-2a-20-50vdc-for-nema-17-23-24-stepper-motor-dm542t, accessed: 10.12.2023.

[18] STEPPERONLINE. P series ip67 waterproof nema 23 stepper motor 5.0 A 1.8 Nm (254.95 oz.in). https://www.omc-stepperonline.com/p-series-ip67-waterproof-nema-23-stepper-motor-5-0a-1-8nm-254-95oz-in-23ip67-20, accessed: 10.12.2023.

[19] Michio Ueno, Hideki Miyazaki, Harukuni Taguchi, Yasushi Kitagawa, and Yoshiaki Tsukada. Reproduction of an actual sea and ship motion using the all-round wave generator. In *OCEANS'11 MTS/IEEE KONA*, pages 1–7, 2011.

[20] J. van der Lucht, M. Bleier, and A. Nüchter. A low cost underwater test environment. *The International Archives of the Photogrammetry, Remote Sensing and Spatial Information Sciences*, XLII-2/W17:399–404, 2019.

[21] Jinhai Zheng, Yu Yao, Songgui Chen, Shubin Chen, and Qiming Zhang. Laboratory study on wave-induced setup and wave-driven current in a 2dh reef-lagoon-channel system. *Coastal Engineering*, 162:103772, 2020.

Proclamation

Hereby I confirm that I wrote this thesis independently and that I have not made use of any other resources or means than those indicated.

Würzburg, January 2024

P. Meyer